

# Hadron Scattering in an Asymmetric Box <sup>1</sup>

China Lattice QCD Collaboration (CLQCD)

Xin Li <sup>a</sup>, Ying Chen <sup>b</sup>, Guo-Zhan Meng <sup>a</sup>, Xu Feng <sup>a</sup>,  
 Ming Gong <sup>a</sup>, Song He <sup>a</sup>, Gang Li <sup>b</sup>, Chuan Liu <sup>a</sup>, Yu-Bin Liu <sup>d</sup>,  
 Jian-Ping Ma <sup>c,a</sup>, Xiang-Fei Meng <sup>d</sup>, Yan Shen <sup>a</sup>,  
 and Jian-Bo Zhang <sup>e</sup>

<sup>a</sup>*School of Physics, Peking University  
 Beijing, 100871, P. R. China*

<sup>b</sup>*Institute of High Energy Physics  
 Academia Sinica, P. O. Box 918  
 Beijing, 100039, P. R. China*

<sup>c</sup>*Institute of Theoretical Physics  
 Academia Sinica, Beijing, 100080, P. R. China*

<sup>d</sup>*Department of Physics, Nankai University  
 Tianjin, 300071, P. R. China*

<sup>e</sup>*Department of Physics, Zhejiang University  
 Hangzhou, 310027, P. R. China*

---

## Abstract

We propose to study hadron-hadron scattering using lattice QCD in an asymmetric box which allows one to access more non-degenerate low-momentum modes for a given volume. The conventional Lüscher's formula applicable in a symmetric box is modified accordingly. To illustrate the feasibility of this approach, pion-pion elastic scattering phase shifts in the  $I = 2, J = 0$  channel are calculated within quenched approximation using improved gauge and Wilson fermion actions on anisotropic lattices in an asymmetric box. After the chiral and continuum extrapolation, we find that our quenched results for the scattering phase shifts in this channel are consistent with the experimental data when the three-momentum of the pion is below 300 MeV. Agreement is also found when compared with previous theoretical results from lattice and other means. Moreover, with the usage of asymmetric volume, we are able to compute the scattering phases in the low-momentum range (pion

three momentum less than about 350MeV in the center of mass frame) for over a dozen values of the pion three-momenta, much more than using the conventional symmetric box with comparable volume.

*Key words:*  $I = 2$ ,  $s$ -wave pion-pion scattering, asymmetric box, scattering phase shift.

*PACS:* 12.38.Gc,11.15.Ha

---

## 1 Introduction

Hadron-hadron scattering experiments have offered us enormous amount of information concerning the interaction among hadrons. In these experiments, scattering cross sections and phase shifts are obtained experimentally in various channels with definite quantum numbers. On the theoretical side, although Quantum Chromodynamics (QCD) has been recognized as the underlying theory of strong interaction, theoretical explanation of hadronic scattering processes at low energies remains a challenging problem due to non-perturbative features of the theory thereof. Lattice QCD (LQCD) is the only systematic, non-perturbative method of QCD which in principle can be applied to calculate these low energy physical quantities from first principles using numerical Monte Carlo simulations. Calculation of hadron-hadron scattering phase shift is also a very important step to deepen our understanding of the strong interaction beyond single hadron spectrum.

Lattice calculation of hadron scattering processes relies on a finite size method proposed by M. Lüscher [1,2,3,4,5] in which two particle elastic scattering phase shifts (in the infinite volume) are directly related to the energy levels of the two particles in a finite cubic box. The latter can in principle be extracted in lattice simulations. Using this technique, the scattering length and the scattering phase shifts for pion-pion scattering in the  $I = 2$ ,  $J = 0$  channel have been studied [6,7,8,9,10,11,12,13,14,15,16] in both quenched and unquenched lattice QCD. There also exist lattice calculations on other hadronic scattering processes using various lattice actions.

---

<sup>1</sup> This work is supported in part by the National Natural Science Foundation of China (NSFC) under grant No. 10421503, No. 10675005, No.10575107, No.10375031, No.10675101 and supported by the Trans-century fund and the Key Grant Project of Chinese Ministry of Education (No. 305001) and KJCX3-SYW-N2 (CAS).

The lattice results on the pion-pion scattering phases can be compared with the experimental data and results from other theoretical methods and impressive agreements were seen [14,15,16]. However, since lattice results were obtained in a finite volume, the number of low-momentum modes accessible for lattice simulation was limited. Part of the reason is that, in all previous lattice studies, hadron scattering phase shifts were calculated in a cubic box which has the same physical extension in all three spatial directions. In this scenario, many low momentum modes are degenerate in energy such as modes  $(1, 0, 0)$ ,  $(0, 1, 0)$  and  $(0, 0, 1)$  since they are related to one another by cubic symmetry. As a result, one can only access very few low-momentum modes in the lattice calculation in a cubic box. If one is interested in the scattering phases at more values of the scattering momenta, larger physical volumes are required which makes the lattice simulation very costly. In this paper, we propose to use asymmetric boxes to study hadron-hadron scattering on the lattice. We test this idea in a quenched study on the pion-pion scattering in the  $I = 2$ ,  $J = 0$  channel. If we denote the three-momentum of each pion in the center of mass frame by  $\bar{k}$ , within the range  $0 < \bar{k}^2 < 0.1\text{GeV}^2$ , we are able to obtain scattering phase shifts at more than 12 different values of  $\bar{k}^2$  while in calculations with comparable cubic volumes this number is restricted to only a few.

This paper is organized as follows. In Section 2, we briefly review the theoretical formalism for the computation of the phase shift in an asymmetric box, extending the finite size technique suggested by Lüscher. The corresponding formulae are modified to the case of asymmetric volume. Possible mixing with the  $J = 2$  channel is discussed. In Section 3, some simulation details are given. Our results for the scattering phases, after chiral and continuum extrapolations, are then compared with known results from previous lattice calculations, chiral perturbation theory, dispersion relations and experimental data. Reasonable agreements are found and the advantage of using the asymmetric box is addressed. In last section, we will summarize this work and give some conclusions and outlooks.

## 2 Lüscher's formulae extended to an asymmetric box

Consider a cubic box with size  $L \times L \times L$  and periodic boundary condition. In such a box, the three momentum of a single pion is quantized as:  $\mathbf{k} = (2\pi/L)\mathbf{n}$  with  $\mathbf{n} = (n_1, n_2, n_3) \in \mathbb{Z}^3$ , where  $\mathbb{Z}$  represents the set of all integers. In this paper, we are interested in two-pion systems. Taking the center of mass reference frame of the two pions, we define  $\bar{\mathbf{k}}^2$  of the pion pair in a box as:

$$E_{\pi\pi} = 2\sqrt{m_\pi^2 + \bar{\mathbf{k}}^2} \quad (1)$$

where  $E_{\pi\pi}$  is the *exact* energy of a two-pion system with the two pions having three momentum  $\mathbf{k}$  and  $-\mathbf{k}$  respectively in the center of mass frame. We further define  $q^2$  via:

$$\bar{\mathbf{k}}^2 = \frac{4\pi^2}{L^2} q^2 \quad (2)$$

Note that, because of the interaction between the two pions in the box, the value of  $q^2$  is in general not equal to  $\mathbf{n}^2$  with  $\mathbf{n} \in \mathbb{Z}^3$ . In fact, in the  $I = 2, J = 0$  channel, the interaction between the two pions is repulsive, making the value of  $q^2$  larger than the corresponding  $\mathbf{n}^2$ .

According to Lüscher's method [4], two-pion  $s$ -wave elastic scattering phase shift can be obtained from the following formula: <sup>2</sup>

$$\cot \delta(\bar{k}) = \frac{\mathcal{Z}_{00}(1, q^2)}{\pi^{3/2} q}, \quad (3)$$

where the so-called zeta function  $\mathcal{Z}_{lm}$  is given by:

$$\mathcal{Z}_{lm}(s, q^2) = \sum_{\mathbf{n}} \frac{\mathcal{Y}_{lm}(\mathbf{n})}{(\mathbf{n}^2 - q^2)^s}. \quad (4)$$

In this definition,  $\mathcal{Y}_{lm}(\mathbf{r}) = r^l Y_{lm}(\Omega_{\mathbf{r}})$ , with  $Y_{lm}(\Omega_{\mathbf{r}})$  being the usual spherical harmonics. When the physical volume is large enough, Lüscher's formula (3) can be expanded as powers of  $1/L$ . The resulting formula then relates the energy level of two hadron in a finite box to the hadron elastic scattering length in the infinite volume. This provides a very convenient way of computing scattering lengths on the lattice. The formula reads:

$$E_{\pi\pi} - 2m_{\pi} = -\frac{4\pi a_0}{m_{\pi} L^3} \left[ 1 + c_1 \left( \frac{a_0}{L} \right) + c_2 \left( \frac{a_0}{L} \right)^2 \right] + O(L^{-6}) \quad (5)$$

where the coefficients  $c_1 = -2.837297$  and  $c_2 = 6.375183$ ,  $a_0$  is the  $\pi\pi$  elastic scattering length.

As explained in the introduction of this paper, many low momentum modes in a cubic box are degenerate in energy due to cubic symmetry. Therefore, to compute the scattering phases at more values of the scattering momenta, one usually has to use larger cubic volumes. This makes the lattice calculation more costly. In this paper, we propose to use an asymmetric volume which provides more non-degenerate low-momentum modes with a relatively small volume. Lüscher's original formula (3) is only valid in a cubic box. To utilize similar finite volume techniques, we must generalize Eq. (3) to the case of an asymmetric box. This has been accomplished in [17,18].

---

<sup>2</sup> This assumes that the contribution from higher angular momentum modes are negligible. In the cubic case, the leading contamination is from  $l = 4$ .

In an asymmetrical box with lattice size  $L \times \eta_2 L \times \eta_3 L$ , the momentum of a single pion is quantized as:  $\mathbf{k} = (2\pi/L)\tilde{\mathbf{n}}$  with  $\tilde{\mathbf{n}} \equiv (n_1, n_2/\eta_2, n_3/\eta_3)$  and  $\mathbf{n} = (n_1, n_2, n_3) \in \mathbb{Z}^3$ . Quantities  $\bar{\mathbf{k}}$  and  $q^2$  are still defined according to Eq. (1) and Eq. (2).

The symmetry group of the asymmetric box depends on the shape of the volume we take in our lattice calculation. For definiteness, we choose  $\eta_2 = 1$  and  $\eta_3 = 2$  in this study and the corresponding basic symmetry group is  $D_4$  which has 4 one-dimensional representations:  $A_1, A_2, B_1, B_2$  and a two-dimensional irreducible representation  $E$ . Rotational symmetry is broken and the corresponding representations for the rotational group with definite angular momentum quantum numbers are decomposed accordingly:

$$\mathbf{0} = A_1^+ , \quad \mathbf{1} = A_2^- + E^- , \quad \mathbf{2} = A_1^+ + B_1^+ + B_2^+ + E^+ , \quad \dots . \quad (6)$$

The formula for the scattering phase shifts is now modified to: <sup>3</sup>

$$\cot \delta(\bar{k}) = m_{00}(q) \equiv \frac{\mathcal{Z}_{00}(1, q^2; \eta_2, \eta_3)}{\pi^{3/2} \eta_2 \eta_3 q} \quad (7)$$

with the modified zeta function  $\mathcal{Z}_{lm}$  defined as:

$$\mathcal{Z}_{lm}(s, q^2; \eta_2, \eta_3) = \sum_{\mathbf{n}} \frac{\mathcal{Y}_{lm}(\tilde{\mathbf{n}})}{(\tilde{\mathbf{n}}^2 - q^2)^s} \quad (8)$$

The formula for scattering length is also changed accordingly:

$$E_{\pi\pi} - 2m_\pi = -\frac{4\pi a_0}{\eta_2 \eta_3 m_\pi L^3} \left[ 1 + c_1(\eta_2, \eta_3) \left(\frac{a_0}{L}\right) + c_2(\eta_2, \eta_3) \left(\frac{a_0}{L}\right)^2 \right] + O(L^{-6}) . \quad (9)$$

where the coefficients  $c_1(\eta_2, \eta_3)$  and  $c_2(\eta_2, \eta_3)$  can be computed once  $\eta_2$  and  $\eta_3$  are given [17]. For the case  $\eta_2 = 1$  and  $\eta_3 = 2$ , which is the situation studied in this paper, the two coefficients are found to be:

$$c_1(1, 2) = -1.805872 , \quad c_2(1, 2) = 1.664979 \quad (10)$$

Therefore, just as in the cubic case, once the two-pion energy level  $E_{\pi\pi}$  is obtained in Monte Carlo simulations, the corresponding phase shift  $\delta$  can be obtained via modified Lüscher's formula (7).

It is noted that the representation  $A_1$  appears in both the  $J = 0$  and  $J = 2$  channel. Therefore, in an asymmetric box,  $s$ -wave and  $d$ -wave scattering mix with each other. This is to be compared with the cubic case where the lowest mixture to  $s$ -wave is from  $l = 4$  sector.

<sup>3</sup> Again, we omit higher angular momentum contributions. In this case, the leading contamination is from  $l = 2$ .

Table 1

Simulation parameters used in this work:

$\beta$	$u_s$	$\nu$	Lattice	$a_s(\text{GeV}^{-1})$	Number of Confs.	$\kappa_{max}$
2.080	0.7735	0.94	$8^2 \times 16 \times 40$	1.5677	464	0.0598
2.215	0.7852	0.95	$9^2 \times 18 \times 48$	1.3926	425	0.0602
2.492	0.8063	0.93	$12^2 \times 24 \times 64$	1.0459	105	0.0606

Assuming the  $d$ -wave scattering phases are small, one can estimate its effect on the  $s$ -wave phase shift as follows [18]:

$$n\pi - \delta_0(q) \simeq \phi(q) + \sigma_2(q) \tan \delta_2(q) , \quad (11)$$

where the angle  $\phi(q)$  is defined via:  $-\tan \phi(q) = 1/m_{00}(q)$ . The function  $\sigma_2(q)$  for  $D_4$  symmetry is given by:

$$\sigma_2(q) = \frac{m_{02}^2(q)}{1 + m_{00}^2(q)} , \quad (12)$$

which quantifies the effect due to  $d$ -wave mixing.<sup>4</sup> On general grounds, one expects the mixing due to higher angular momentum to be small in the low-momentum region. To estimate its effect in the case of pion-pion scattering, we take experimental values for the  $d$ -wave scattering phases presented in Ref. [19]. We have checked this correction to our  $s$ -wave phase shifts and it is found that these corrections are only of about 1 – 2%, much smaller than our typical error bars for the phase shifts. Therefore, in what follows, we simply neglect the effects of the  $d$ -wave contaminations.

### 3 Simulation Details

To test our idea of using the asymmetric box on hadron-hadron scattering, we perform a quenched study on the pion-pion scattering phase shift in the  $I = 2$ ,  $J = 0$  channel. In this section, we will briefly introduce our numerical results.

#### 3.1 Lattice actions and simulation parameters

The gauge action used in this study is the tadpole improved gluonic action on anisotropic lattices [20,21]:

$$S = -\beta \sum_{i>j} \left[ \frac{5}{9} \frac{\text{Tr} P_{ij}}{\xi u_s^4} - \frac{1}{36} \frac{\text{Tr} R_{ij}}{\xi u_s^6} - \frac{1}{36} \frac{\text{Tr} R_{ji}}{\xi u_s^6} \right]$$

<sup>4</sup> The explicit formula for the function  $m_{02}(q)$  can be found in Ref. [18].

$$- \beta \sum_i \left[ \frac{4}{9} \frac{\xi \text{Tr} P_{0i}}{u_s^2} - \frac{1}{36} \frac{\xi \text{Tr} R_{i0}}{u_s^4} \right] \quad (13)$$

where  $P_{ij}$  is the usual spatial plaquette variables and  $R_{ij}$  is the  $2 \times 1$  spatial Wilson loop on the lattice. The parameter  $u_s$ , which we take to be the 4-th root of the average spatial plaquette value, incorporates the so-called tadpole improvement [22] and  $\xi$  designates the (bare) aspect ratio of the anisotropic lattice, defined as the ratio between two spacings  $a_s/a_t$ . With the tadpole improvement, experiences show that the renormalization effects are small for this parameter. Thus, we have not distinguish the renormalized anisotropy and the bare one. The anisotropic and improvement property of the lattice action makes the calculation of heavier hadronic objects on coarser lattice possible. The parameter  $\beta$  is related to the bare gauge coupling which controls the spatial lattice spacing  $a_s$  in physical units. This type of improved gauge action on anisotropic lattices have been extensively used in lattice calculations on glueballs [21,23,24,25,26].

The fermion action used in this calculation is the tadpole improved clover Wilson action on anisotropic lattice [27,28,29] whose fermion matrix reads:  $\mathcal{M}_{xy} = \delta_{xy}\sigma + \mathcal{A}_{xy}$  with  $\mathcal{A}$  given by:

$$\begin{aligned} \mathcal{A}_{xy} = & \delta_{xy} [1/(2\kappa_{max}) + \rho_t \sum_{i=1}^3 \sigma_{0i} \mathcal{F}_{0i} + \rho_s (\sigma_{12} \mathcal{F}_{12} + \sigma_{23} \mathcal{F}_{23} + \sigma_{31} \mathcal{F}_{31})] \\ & - \sum_{\mu} \eta_{\mu} [(1 - \gamma_{\mu}) U_{\mu}(x) \delta_{x+\mu,y} + (1 + \gamma_{\mu}) U_{\mu}^+(x - \mu) \delta_{x-\mu,y}] \end{aligned} \quad (14)$$

where the coefficients are given by:

$$\begin{aligned} \eta_i = & \nu/(2u_s), \eta_0 = \xi/2, \sigma = 1/(2\kappa) - 1/(2\kappa_{max}), \\ \rho_t = & c_{SW}(1 + \xi)/(4u_s^2), \rho_s = c_{SW}/(2u_s^4). \end{aligned} \quad (15)$$

In this notation, the fermion propagators with different quark masses could be solved at the same time using the so-called Multi-mass Minimal Residual ( $M^3R$ ) algorithm [30,31,32]. The bare velocity of light parameter  $\nu$  is tuned non-perturbatively using the single pion dispersion relations [29,33]. The parameters  $\kappa_{max}$  is the largest one among all  $\kappa$  parameters which corresponds to the lightest valence quark mass. The asymmetrical ratio  $\xi$  is always fixed at  $\xi = 5$ . Other parameters in our simulation are tabulated in Table 1.

Quenched configurations are generated using the pure gauge action (3.1) with three lattice sizes,  $8^2 \times 16 \times 40$ ,  $9^2 \times 18 \times 48$  and  $12^2 \times 24 \times 64$ , corresponding to  $\beta = 2.080$ ,  $2.215$  and  $2.492$ , respectively. The values of  $\beta$  are chosen such that the physical volumes for these three lattices remain the same. The correspondence of  $\beta$  and the spatial lattice spacing  $a_s$  has been obtained in Ref. [34]. The physical volume of our lattices is about  $5.5 fm^3$  which is large

enough to bring the finite volume errors under control. For each set of parameters, several hundreds of de-correlated gauge configurations are utilized to measure physical quantities.

### 3.2 Hadronic operators and the extraction of one and two pion energies

To obtain energy levels for the single and two-pion systems on the lattice, we have to construct appropriate correlation functions using the corresponding hadronic operators. In this paper, single and two pion operators are constructed using local quark fields. For the single pion operators, we use:

$$\begin{aligned}\pi^+(\mathbf{x}, t) &= -\bar{d}(\mathbf{x}, t)r_5u(\mathbf{x}, t), \pi^-(\mathbf{x}, t) = \bar{u}(\mathbf{x}, t)r_5d(\mathbf{x}, t) \\ \pi^0(\mathbf{x}, t) &= \frac{1}{\sqrt{2}}(\bar{u}(\mathbf{x}, t)r_5d(\mathbf{x}, t) - \bar{d}(\mathbf{x}, t)r_5u(\mathbf{x}, t))\end{aligned}\quad (16)$$

where  $u(\mathbf{x}, t)$  and  $d(\mathbf{x}, t)$  are the basic local quark field operators for the up and down quark, respectively. In this study, the up and down quarks are taken to be degenerate in mass so that isospin is a good symmetry. The operator which creates a single pion with non-zero three momentum  $\mathbf{k}$  from the vacuum is obtained by Fourier transform:

$$\pi_{\mathbf{k}}^a(t) = \frac{1}{V_3} \sum_{\mathbf{x}} \pi^a(\mathbf{x}, t) e^{-i\mathbf{k}\cdot\mathbf{x}} \quad (17)$$

where the flavor index  $a$  of pions take values  $a = +, -, 0$  and  $V_3$  is the three volume of the lattice. By calculating correlation functions of single pion operators defined above, one can obtain the single pion energy at vanishing and non-vanishing momenta.

The  $s$ -wave two-pion operators in the  $I = 2$  channel are defined as:

$$\mathcal{O}_n(t) = \sum_R \pi_{R(\mathbf{k}_n)}^+(t) \pi_{R(-\mathbf{k}_n)}^+(t+1), \quad (18)$$

where  $n$  labels a particular mode with three-momentum  $\mathbf{k}_n$ ;  $R(\mathbf{k}_n)$  is the rotated three-momentum which is obtained from  $\mathbf{k}_n$  by applying a symmetry operation  $R \in D_4$ , an element of the corresponding point group. Therefore, the summation of  $R$  in Eq. (18) guarantees that the operator thus constructed falls into the  $A_1^+$  representation of the symmetry group whose continuum counterpart is  $s$ -wave for the rotational group, if the contaminations from the  $l \geq 2$  sectors are negligible.

In order to obtain the two-pion energies, which is directly related to the scattering phases we want to compute, we measure the correlation matrix among different non-degenerate two-pion



Table 2

The representative momentum of every mode. Mode 2, 4 and 5 have accidental degenerate modes which are left out in the construction of two pion operators.

Serial Number	0	1	2	3	4	5	6
Mode $\tilde{\mathbf{n}}$	(0,0,0)	(0,0,1/2)	(1,0,0)	(1,0,1/2)	(1,1,0)	(1,1,1/2)	(1,1,1)
Degenerate Mode $\tilde{\mathbf{n}}$			(0,0,1)		(1,0,1)	(0,0,3/2)	

modes, using the two-pion operators defined in Eq. (18):

$$\mathcal{C}_{mn}(t) = \langle \mathcal{O}_m^\dagger(t) \mathcal{O}_n(t_s) \rangle . \quad (19)$$

We then follow Lüscher and Wolff's suggestion and constructed a new correlation matrix:

$$\Omega(t, t_0) = \mathcal{C}(t_0)^{-\frac{1}{2}} \mathcal{C}(t) \mathcal{C}(t_0)^{-\frac{1}{2}} \quad (20)$$

where  $t_0$  is some suitable reference time. The eigenvalue  $\lambda_i(t)$  of this new matrix  $\Omega$  is:

$$\lambda_i(t, t_0) \propto e^{-E_i(t-t_0)} \quad (21)$$

It can be shown that [3] this eigenvalue avoids  $\mathcal{O}(e^{-\Delta Et})$  errors and the energy eigenvalues could be extracted by a single exponential in  $t$ . We choose seven non-degenerate momentum modes to construct the correlation function matrix (19). The representative momentum of each non-degenerate momentum mode is tabulated in Table 2. Note that some modes might become accidentally degenerate in the continuum limit when rotational invariance is completely restored. That is to say, two modes are degenerate in energy in the continuum limit but they are not related to one another by any  $D_4$  transformation. In Table 2 we also list these accidental degenerate modes. Although for finite lattice spacings, scaling violations will lift these degeneracies, the almost degenerate modes might make the diagonalization procedure unstable. Therefore, in our study of the two-pion correlation matrix, the accidental degenerate modes are left out in the construction of the two-pion operators.

The single pion correlations at zero spacial momentum are constructed from the wall source quark propagators. Effective mass functions are then used to extract the single pion mass values. The mass plateaus are determined automatically by requiring the minimal of  $\chi^2$  per degree of freedom. All effective mass plateaus are plotted in Fig. 1. The horizontal line segments in these figures represent the ranges of the plateaus from which the pion masses are extracted. The errors for the data points are obtained from a standard jack-knife analysis.

Similar analysis is performed for the two-pion correlation matrix. It is verified that the symmetric off-diagonal matrix elements,  $\mathcal{C}_{ij}$  and  $\mathcal{C}_{ji}$  ( $i \neq j$ ) of the matrix, are almost equal to each other in all cases except for some high modes at large time slices. Therefore, in our analysis,  $\mathcal{C}_{ij}$  and  $\mathcal{C}_{ji}$  ( $i \neq j$ ) are simply averaged to construct a symmetric positive-definite matrix. In

Table 3

Chiral extrapolation fits of  $\frac{a_0}{m_\pi}$  using Scheme 1 and the continuum limit of the fitted parameter  $A_0$  (the corresponding value in the chiral limit).

$\beta$	$A_0$ (GeV $^{-2}$ )	$A_1$ (GeV $^{-4}$ )	$\chi^2/d.o.f$	range
2.080	-2.30(15)	0.44(16)	0.05	1–12
2.215	-2.27(14)	0.59(17)	0.04	1–8
2.492	-2.15(19)	0.82(20)	0.09	1–4
continuum limit	-2.05(36)			
$\chi^2/d.o.f$	0.18			

Table 4

Chiral extrapolation of  $\frac{a_0}{m_\pi}$  at  $\beta = 2.492$  using Scheme 2. With others still using Scheme 1, the continuum limit of parameter  $A_0$  is shown.

$\beta$	$A_0$ (GeV $^{-2}$ )	$A_1$ (GeV $^{-4}$ )	$A_2$ (GeV $^{-6}$ )	$\chi^2/d.o.f$	range
2.492	-2.24(16)	1.15(21)	-2.24(6)	0.13	1–12
continuum limit	-2.20(30)				
$\chi^2/d.o.f$	0.02				

the diagonalization procedure, we set  $t_0 = 3$  as the reference time. The effective energies of two-pion energy levels are defined as  $E_{\pi\pi}(i, t) = \ln(\frac{\lambda_i(t)}{\lambda_i(t+1)})$  where the index  $i$  represents the  $i$ -th eigenmode and the energy plateaus  $E_{\pi\pi}$  are found accordingly. In Fig. 2, the effective mass plateaus at  $\beta = 2.492$  for various modes are shown. Data for other values of  $\beta$  are similar. The corresponding values for  $\bar{\mathbf{k}}$  can thus be obtained from Eq. (1) and the values for  $\delta$  may be computed by Eq. (7) for each set of bare parameters.

### 3.3 Results for the scattering length

It is found that the relative three momentum  $|\bar{\mathbf{k}}|$  for Mode 0 is far smaller than the corresponding single-pion mass values. Therefore,  $\delta E = E_{\pi\pi} - 2m_\pi$  can be obtained from Mode 0 ignoring the small three momentum effect. It is then easy to obtain the scattering length  $a_0$  in this channel using formula (9) for every valence quark mass and  $\beta$  value. These results are then used to perform the chiral extrapolation.

We use the quantity  $a_0/m_\pi$ , which is finite in the chiral limit, for the chiral extrapolation, as suggested by the CP-PACS collaboration [14]. The scale is set using the pure gauge sector with the Sommer scale  $r_0 = 0.5\text{fm}$ . In Chiral perturbation Theory (ChPT), The  $m_\pi^2$  dependence of the scattering length is known within Chiral perturbation theory (ChPT) [35,36,37]. However, it is well-known that ChPT is only effective when  $m_\pi$  is small. The pion mass range in our simulation (from 0.7 GeV to 1.5 GeV) is definitely beyond the applicability range of ChPT. Therefore, we have attempted to parameterize our data for  $a_0/m_\pi$  using either a linear function

Table 5

A summary of results for the pion-pion scattering length.

	$a_0 m_\pi$		$a_0 m_\pi$
JLQCD (LIN)[8]	-0.0406(47)	CP-PACS (quenched) [14]	-0.0558(56)
JLQCD (EXP)[8]	-0.0410(69)	E865 Collaboration [41]	-0.036(9)
C.Liu (Scheme 1)[10]	-0.0342(75)	Current algebra [38]	-0.046
C.Liu (Scheme 2)[10]	-0.0459(91)	CHPT (one-loop) [39]	-0.0423(10)
X.Du[12]	-0.0467(45)	CHPT (two-loop, Roy Eq.) [37]	-0.0444(10)
CP-PACS (unquenched) [15]	-0.0266(16)	Dispersion relations [40]	-0.0440(11)

in  $m_\pi^2$ :

$$\frac{a_0}{m_\pi} = A_0 + A_1 m_\pi^2; , \quad (22)$$

or a quadratic function in  $m_\pi^2$ :

$$\frac{a_0}{m_\pi} = A_0 + A_1 m_\pi^2 + A_2 m_\pi^4 . \quad (23)$$

These two methods will be referred to as Scheme 1 and 2. It is found that only the data at  $\beta = 2.492$  show significant curvature in the pion mass regime that we are studying. For the other two  $\beta$  values, quadratic fits do not give statistically more favorable results. Therefore, we only attempted Scheme 2 for  $\beta = 2.492$ . The fitting results in both schemes are tabulated in Table 3 and Table 4. The fittings are also illustrated in the left panels of Fig. 3 and Fig. 4.

Finally, a continuum limit extrapolation is performed to get rid of the lattice spacing errors, using a functional form that is linear in  $a_s^2$ . A possible linear term contamination might be there but the coefficient of it is too small to be visible in the fitting. In Fig. 3 and Fig. 4 (right panels), we show the results for the continuum limit extrapolation. The straight lines represent the extrapolation towards the  $a_s = 0$  limit and the final results are shown as circles. After the chiral and continuum extrapolations, our results for the scattering length in this particular channel read:

$$a_0 m_\pi = \begin{cases} 0.0399(70) , & \text{Scheme 1} \\ 0.0359(59) , & \text{Scheme 2} \end{cases} \quad (24)$$

The two results are consistent with each other within errors. These results can also be compared with analogous results obtained in other theoretical calculations [38,39,37,40] and the experiment [41]. Our results of two schemes are both compatible with the experiment and the result of Scheme 1 is consistent with the results from other theoretical investigations. Our result for the scattering length also agrees with previous lattice results obtained by other groups. Table 5 summarizes all relevant results for the scattering length in this channel.

### 3.4 The scattering phase shift

We now come to the results for scattering phases. Pion scattering phases can also be computed in the low-energy regime within chiral perturbation theory [35,36]. However, as already mentioned above, the formulae thus obtained are only applicable for very light pion mass and low scattering momenta. We therefore used a method that has been used in quenched studies by the CP-PACS Collaboration [14,42,15], namely we simply parameterize the scattering phases with a polynomial in  $m_\pi^2$  and the momentum. Our method is a modified version of their methods.

CP-PACS Collaboration [14,42,15] defines a scattering amplitude as follows:

$$A(m_\pi, \bar{k}) = \frac{\tan \delta(\bar{k})}{\bar{k}} \cdot \frac{E_{\pi\pi}}{2} \quad (25)$$

where  $\bar{k} = |\bar{\mathbf{k}}|$ . Then, they used a polynomial function in both  $m_\pi^2$  and  $\bar{k}^2$  to fit their simulation data. However, if some of the phase shifts data exceeded the limit  $-90^\circ$ , since the function  $A(m_\pi, \bar{k})$  defined above involves the tan function which is discontinuous at  $-90^\circ$ , this makes the amplitude  $A(m_\pi, \bar{k})$  discontinuous as well which is not convenient for chiral extrapolations. To overcome this difficulty, we parameterize the phase shift  $\delta$  itself by a polynomial in both  $m_\pi^2$  and  $\bar{k}^2$  as:

$$\delta(m_\pi^2, \bar{k}^2) = D_{00} + D_{10}m_\pi^2 + D_{20}m_\pi^4 + D_{01}\bar{k}^2 + D_{11}m_\pi^2\bar{k}^2 + D_{02}\bar{k}^4 \quad (26)$$

The above function includes all terms with powers not larger than four. We have tried polynomial functions with higher powers but found that they had not improved the fitting quality. Note that in quenched lattice QCD, since the chiral behavior is different from true QCD, physical quantities can suffer from bad chiral behaviors [43]. For example, in the above fitting formulae, a non-vanishing constant term  $D_{00}$  can exist, which would be absent in true QCD due to chiral symmetry. In practice, by fitting of our quenched data, we find that  $D_{00}$  is always consistent with zero within statistical error when we regard it as a free parameter. Therefore, in the following discussion  $D_{00}$  is fixed to zero.

All fitting results for  $D_{ij}$  are tabulated in Table 6. The  $\chi^2/d.o.f$  of  $\beta = 2.215$  is somewhat large but still acceptable. In Fig. 6, we plot the fitted results for the phase shift  $\delta$  as a function of momentum  $\bar{k}^2$  while setting  $m_\pi$  to zero (chiral limit). Results for three  $\beta$  values are all shown in this figure with different symbols. The results for different lattice spacings tend to agree with one another in the low-momentum limit and deviate in the large momentum limit as expected. We then perform the continuum limit extrapolation of various coefficients  $D_{ij}$  by using a function linear in  $a_s^2$ . All extrapolations tabulated in Table 6 are good except for  $D_{02}$ .

Table 6

Fitted results for the scattering phase shifts  $\delta$  at each  $\beta$ . The continuum limit for each parameter is also shown.

$\beta$	$D_{10}$ (GeV <sup>2</sup> )	$D_{20}$ (GeV <sup>4</sup> )	$D_{01}$ (GeV <sup>2</sup> )	$D_{11}$ (GeV <sup>4</sup> )	$D_{02}$ (GeV <sup>4</sup> )	$\chi^2/\text{d.o.f}$
2.080	-24.8(33)	10.9(19)	-165(11)	-133.8(96)	259(16)	0.98
2.215	-18.8(23)	6.7(19)	-161.2(74)	-104.8(61)	190.8(99)	2.05
2.492	-11.6(19)	3.42(91)	-191.3(92)	-69.5(36)	252(12)	0.77
continuum limit	-1.4(41)	-1.9(25)	-213(19)	-20.2(92)	254(25)	

The continuum extrapolations are also shown in Fig. 5. After the continuum extrapolation, the results for the phase shift as a function of  $\bar{\mathbf{k}}^2$  are plotted in Fig. 6 with upside-down triangles.

Our results can be compared with previous quenched lattice results from CP-PACS collaborations [14] and unquenched results from NPLQCD [16]. We find that they agree with each other within errors. Due to the asymmetric box used in this study, we are able to compute the phase shifts at more values of scattering momentum compared with similar calculations using a symmetric box. For example, in Ref. [14], scattering phases are obtained at five values of  $\bar{\mathbf{k}}^2$  in the range from 0.02GeV<sup>2</sup> to 0.34GeV<sup>2</sup>. By using an asymmetric box, even in a smaller range of 0.02GeV<sup>2</sup> to 0.12GeV<sup>2</sup>, we have over a dozen of data points for the phase shift which can be compared with results from other theoretical investigations and the experiments in more detail.

Finally in Fig. 7, we have shown the the same result for the phase shifts  $\delta$  in the continuum limit together with the experimental results from CERN-Munich group [19]. It is seen that our final results agree with the experimental results within errors for  $\bar{\mathbf{k}}^2$  below 0.1 GeV<sup>2</sup> which is about  $\sqrt{s} = 0.6$  GeV. At higher energies, our results deviate from the experimental results. This deviation might be caused by the systematic uncertainties in our calculation, e.g. quenching and chiral extrapolations. Numerically speaking, it is largely due to poor determination of the coefficient  $D_{02}$ . However, we would like to point out that, it is clear from our quenched calculation that, the asymmetric volume technique advocated here would also be useful for unquenched studies once the unquenched configurations become available.

## 4 Conclusions

In this paper, we propose to study hadron-hadron scattering processes on lattices with asymmetric volume. This setup has the advantage that it provides much more non-degenerate low-momentum modes with a relatively small volume, allowing more detailed comparison

both with the experiments and with other theoretical results. To illustrate the feasibility of this proposal, pion pion scattering length and scattering phases in the  $I = 2, J = 0$  channel are computed within quenched lattice QCD using clover improved lattice actions on anisotropic lattices. Our quenched results indicate that the usage of asymmetric volumes indeed allow us to access much more low-momentum modes than in the case of cubic volume of similar size. For  $\bar{k}^2$  in the range of  $0.02\text{GeV}^2$  to  $0.12\text{GeV}^2$ , we have over a dozen of data points for the phase shift, much more than that in the cubic case with similar volume. It is also noted that, in the low-momentum region, after the chiral and continuum extrapolations, our results for the scattering length and the scattering phase shifts are in good agreement with the experimental data and are consistent with results obtained using other theoretical means.

Although our calculation is now performed in the quenched approximation, similar calculations are also possible in the unquenched case once the gauge field configurations become available. Finally, we have only computed scattering length and phases in the  $I = 2, J = 0$  channel. Phenomenologically speaking, other channels, in particular  $I = J = 0$  channel, are more interesting. However, this channel is difficult for two main reasons: One needs to perform a full QCD calculation otherwise the theory is sick in the chiral limit [43]; one has to deal with vacuum (disconnected) diagrams which significantly increase the amount of computational cost. Also interesting and equally challenging is the  $I = J = 1$  channel where one would expect to see a rho resonance [44]. We expect the use of asymmetric volumes should also be beneficial in these studies since a lot more low-momentum modes become accessible in an asymmetric box.

## Acknowledgments

The authors would like to thank Prof. H. Q. Zheng and Prof. S. L. Zhu of Peking University for helpful discussions. The numerical calculations were performed on DeepComp 6800 supercomputer of the Supercomputing Center of Chinese Academy of Sciences, Dawning 4000A supercomputer of Shanghai Supercomputing Center, and NKstar2 Supercomputer of Nankai University.

## References

- [1] M. Lüscher. Volume dependence of the energy spectrum in massive quantum field theories. 1. stable particle states. *Commun. Math. Phys.*, 104:177, 1986.

- [2] M. Lüscher. Volume dependence of the energy spectrum in massive quantum field theories. 2. scattering states. *Commun. Math. Phys.*, 105:153, 1986.
- [3] M. Lüscher and U. Wolff. How to calculate the elastic scattering matrix in two-dimensional quantum field theories by numerical simulation. *Nucl. Phys. B*, 339:222, 1990.
- [4] M. Lüscher. Two particle states on a torus and their relation to the scattering matrix. *Nucl. Phys. B*, 354:531, 1991.
- [5] M. Lüscher. Signatures of unstable particles in finite volume. *Nucl. Phys. B*, 364:237, 1991.
- [6] R. Gupta, A. Patel, and S. Sharpe. I=2 pion scattering amplitude with wilson fermions. *Phys. Rev. D*, 48:388, 1993.
- [7] M. Fukugita, Y. Kuramashi, H. Mino, M. Okawa, and A. Ukawa. Hadron scattering lengths in lattice qcd. *Phys. Rev. D*, 52:3003, 1995.
- [8] S. Aoki et al. I=2 pion scattering length with wilson fermions. *Nucl. Phys. (Proc. Suppl.) B*, 83:241, 2000.
- [9] S. Aoki et al. I=2 pion scattering length with the wilson fermions. *Phys. Rev. D*, 66:077501, 2002.
- [10] C. Liu, J. Zhang, Y. Chen, and J.P. Ma. Calculating the i=2 pion scattering length using tadpole improved clover wilson action on coarse anisotropic lattices. *Nucl. Phys. B*, 624:360, 2002.
- [11] P. Hasenfratz, K.J. Juge, and F. Niedermayer. New results on cut-off effects in spectroscopy with the fixed point action. *JHEP*, 0412:030, 2004.
- [12] X. Du, G. Meng, C. Miao, and C. Liu.  $i = 2$  pion scattering length with improved actions on anisotropic lattices. *Int. J. Mod. Phys. A*, 19:5609, 2004.
- [13] S. Aoki et al. I=2 pion scattering length from two-pion wave functions. *Phys. Rev. D*, 71:094504, 2005.
- [14] S. Aoki et al. I=2 pion scattering phase shift with wilson fermions. *Phys. Rev. D*, 67:014502, 2003.
- [15] T. Yamazaki et al. I=2  $\pi\pi$  scattering phase shift with two flavors of o(a) improved dynamical quarks. *Phys. Rev. D*, 70:074513, 2004.
- [16] Silas R. Beane, Paulo F. Bedaque, Kostas Orginos, and Martin J. Savage. I=2 pi-pi scattering from fully-dynamical mixed-action lattice qcd. *Phys. Rev. D*, 73:054503, 2006.
- [17] X. Li and C. Liu. Two particle states in an asymmetric box. *Phys. Lett. B*, 587:100, 2004.
- [18] X. Feng, X. Li, and C. Liu. Two particle states in an asymmetric box and the elastic scattering phases. *Phys. Rev. D*, 70:014505, 2004.

- [19] W. Hoogland et al. Isospin-two pi pi phase shifts from an experiment  $\pi^+ p \rightarrow \pi^+ \pi^+ n$  at 12.5 gev/c. *Nucl. Phys.*, B69:266–278, 1974.
- [20] C. Morningstar and M. Peardon. Efficient glueball simulations on anisotropic lattices. *Phys. Rev. D*, 56:4043, 1997.
- [21] C. Morningstar and M. Peardon. The glueball spectrum from an anisotropic lattice study. *Phys. Rev. D*, 60:034509, 1999.
- [22] G. P. Lepage and P. B. Mackenzie. On the viability of lattice perturbation theory. *Phys. Rev. D*, 48:2250, 1993.
- [23] C. Liu. A lattice study of the glueball spectrum. *Chinese Physics Letter*, 18:187, 2001.
- [24] C. Liu. A lattice study of the glueball spectrum. *Communications in Theoretical Physics*, 35:288, 2001.
- [25] C. Liu. Scalar and tensor glueball spectrum on anisotropic lattices. *Nucl. Phys. (Proc. Suppl.) B*, 94:255, 2001.
- [26] Y. Chen, A. Alexandru, S.J. Dong, T. Draper, I. Horvath, F.X. Lee, K.F. Liu, N. Mathur, C. Morningstar, M. Peardon, S. Tamhankar, B.L. Young, and J.B. Zhang. Glueball spectrum and matrix elements on anisotropic lattices. *Phys. Rev. D*, 73:014516, 2006.
- [27] M. Alford, T. R. Klassen, and P. Lepage. A quark action for very coarse lattices. *Phys. Rev. D*, 58:034503, 1998.
- [28] T. R. Klassen. Non-perturbative improvement of the anisotropic wilson qcd action. *Nucl. Phys. (Proc. Suppl.) B*, 73:918, 1999.
- [29] Junhua Zhang and C. Liu. Tuning the tadpole improved clover wilson action on coarse anisotropic lattices. *Mod. Phys. Lett. A*, 16:1841, 2001.
- [30] A. Frommer, S. Güsken, T. Lippert, B. Nöckel, and K. Schilling. Many masses on one stroke: Economic computation of quark propagators. *Int. J. Mod. Phys. C*, 6:627, 1995.
- [31] U. Glaessner, S. Guesken, T. Lippert, G. Ritzenhoefer, K. Schilling, and A. Frommer. How to compute green’s functions for entire mass trajectories within krylov solvers. *hep-lat/9605008*.
- [32] B. Jegerlehner. Krylov space solvers for shifted linear systems. *hep-lat/9612014*.
- [33] Shiquan Su, Liuming Liu, Xin Li, and Chuan Liu. A numerical study of improved quark actions on anisotropic lattices. *Int. J. Mod. Phys. A*, 21:1015, 2006.
- [34] Wei Liu, Ying Chen, Ming Gong, Xin Li, GuoZhan Meng, and Chuan Liu. Static quark potential and the renormalized anisotropy on tadpole improved anisotropic lattices. *Mod. Phys. Lett. A*, 21:2313, 2006.



- [35] J. Gasser and H. Leutwyler. Chiral perturbation theory to one loop. *Annals of Physics*, 158:142, 1984.
- [36] J. Gasser and H. Leutwyler. Chiral perturbation theory: Expansion in the mass of the strange quark. *Nucl. Phys. B*, 250:465, 1985.
- [37] G. Colangelo, J. Gasser, and H. Leutwyler.  $\pi\pi$  scattering. *Nucl. Phys. B*, 603:125, 2001.
- [38] S. Weinberg. *Phys. Rev. Lett.*, 17:616, 1966.
- [39] J. Bijnens, G. Colangelo, and P. Talavera. *JHEP*, 9805:014, 1998.
- [40] Z. Y. Zhou, G. Y. Qin, P. Zhang, Z. G. Xiao, H. Q. Zheng, and N. Wu. The pole structure of the unitary, crossing symmetric low energy  $\pi\pi$  scattering amplitudes. *JHEP*, 0502:043, 2005.
- [41] S. Pislak et al. A new measurement of  $k_{e4}$  decay and the s-wave pi-pi-scattering length  $a_0$ . *Phys. Rev. Lett.*, 87:221801, 2001.
- [42] T. Yamazaki et al. I=2 pion-pion scattering phase shift in the continuum limit calculated with two-flavor full qcd. *hep-lat/0309155*, 2003.
- [43] Claude W. Bernard and Maarten F. L. Golterman. Finite volume two pion energies and scattering in the quenched approximation. *Phys. Rev.*, D53:476–484, 1996.
- [44] CP-PACS collaboration.  $\rho$  meson decay from the lattice. *POS (LAT2006)*, page 110, 2006.

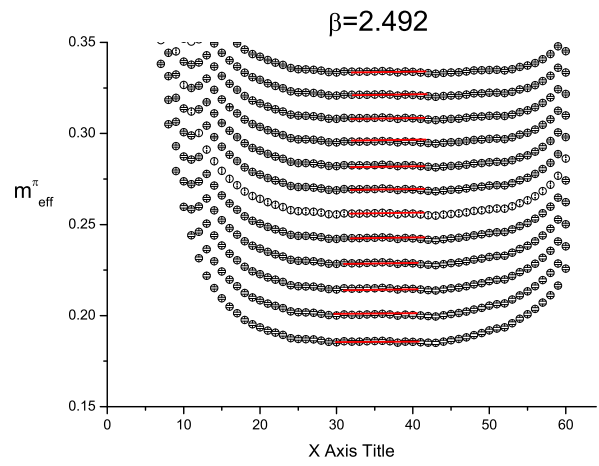
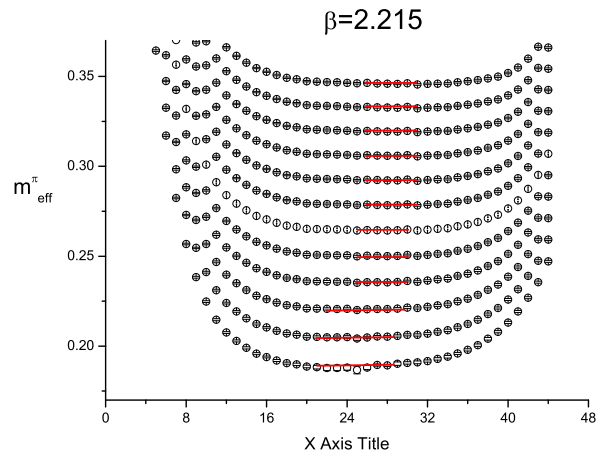
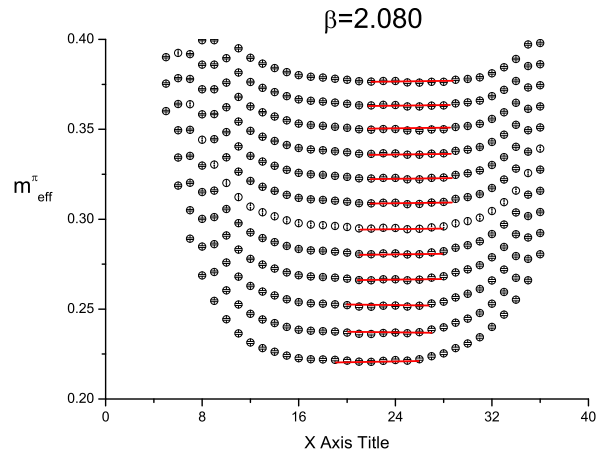


Fig. 1. The single pion effective mass plateaus are shown. The horizontal line segments in the figure represent the fitting ranges of the plateaus.

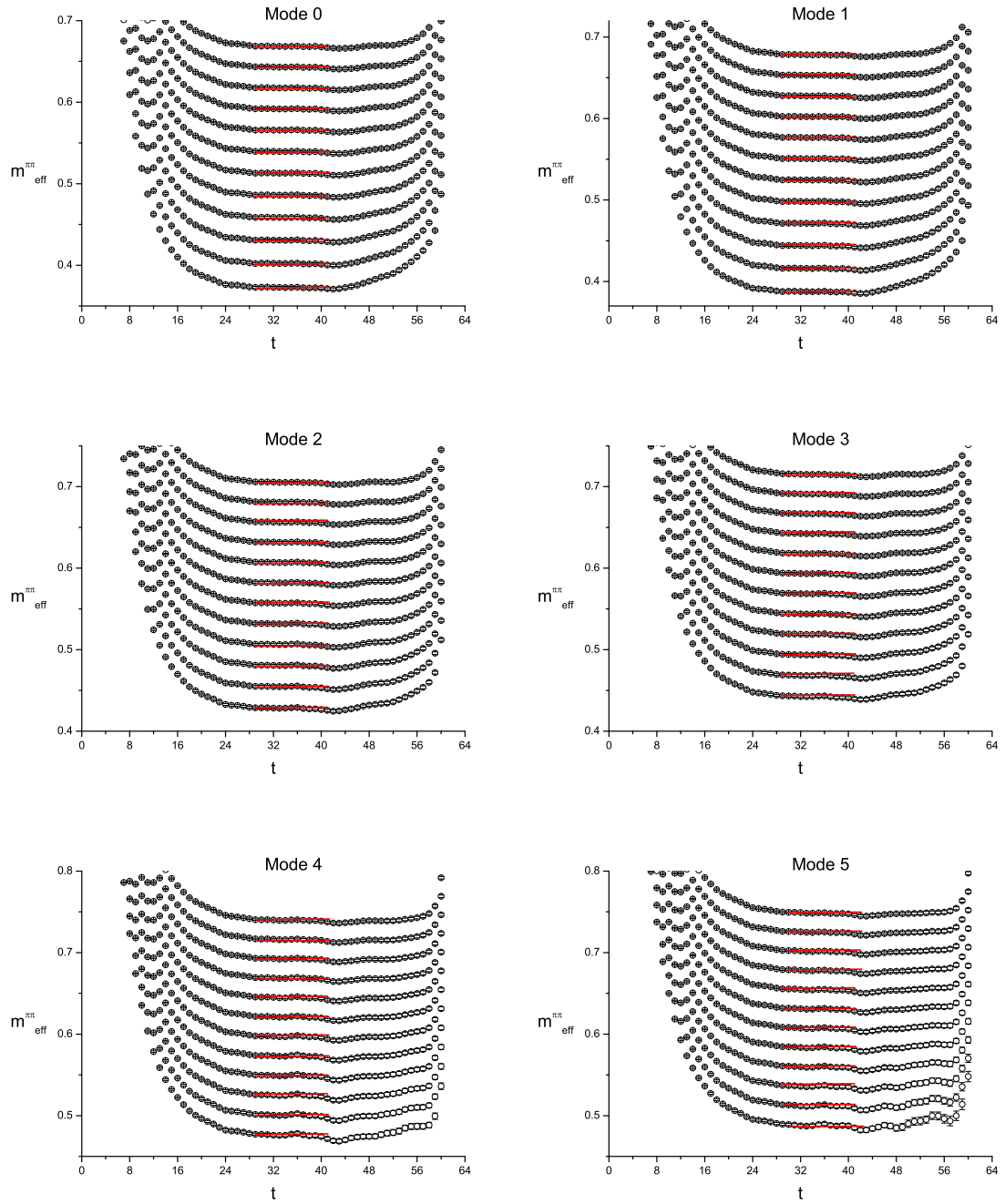


Fig. 2. Effective mass plateaus of two-pion system at  $\beta = 2.492$  after the diagonalization procedure. The horizontal line segments in the figure represent the fitting ranges of the plateaus. Results for other values of  $\beta$  are similar.

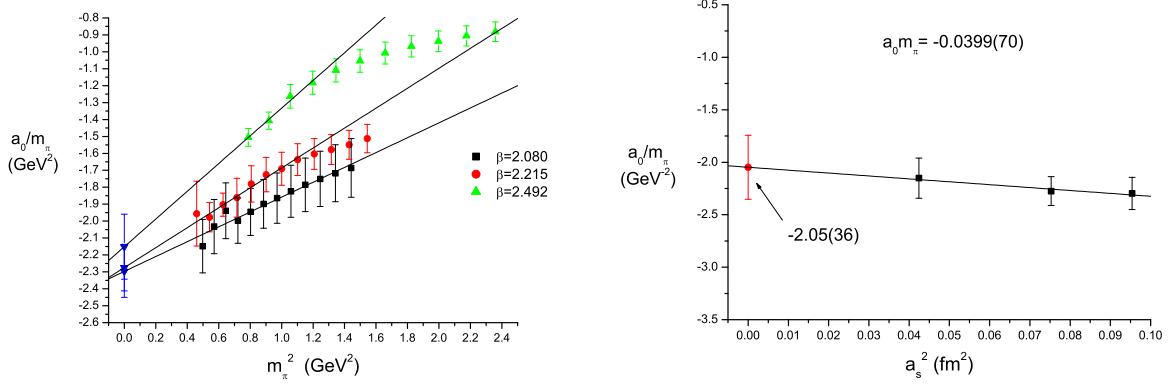


Fig. 3. Left panel: chiral extrapolation of the quantity  $\frac{a_0}{m_\pi}$  using Scheme 1 as described in the paper. Right panel: the corresponding continuum limit extrapolation of the quantity  $\frac{a_0}{m_\pi}$ . The extrapolated result is indicated by a solid circle near  $a_s = 0$ .

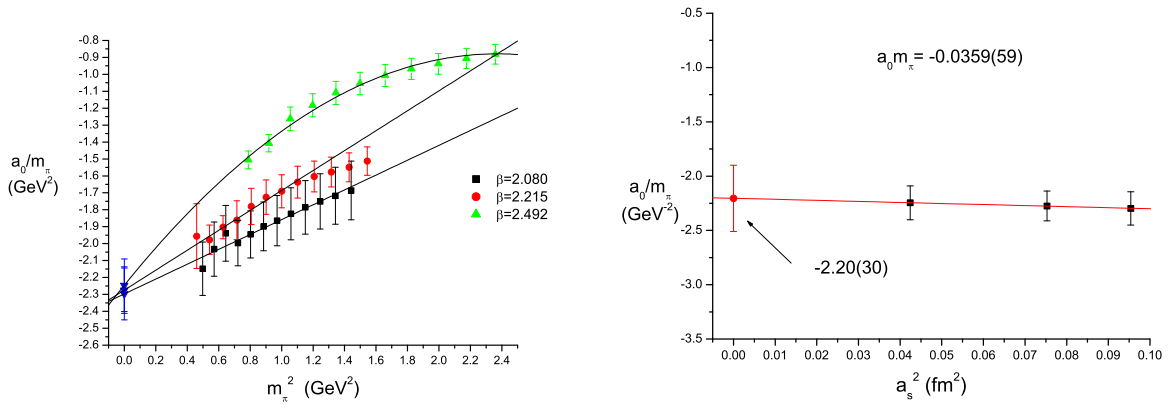


Fig. 4. Left panel: chiral extrapolation of  $\frac{a_0}{m_\pi}$  at  $\beta = 2.492$  using Scheme 2 while keeping other beta values extrapolated in Scheme 1. Right panel: the corresponding continuum limit extrapolation of the quantity  $\frac{a_0}{m_\pi}$ . The extrapolated result is indicated by a solid circle near  $a_s = 0$ .

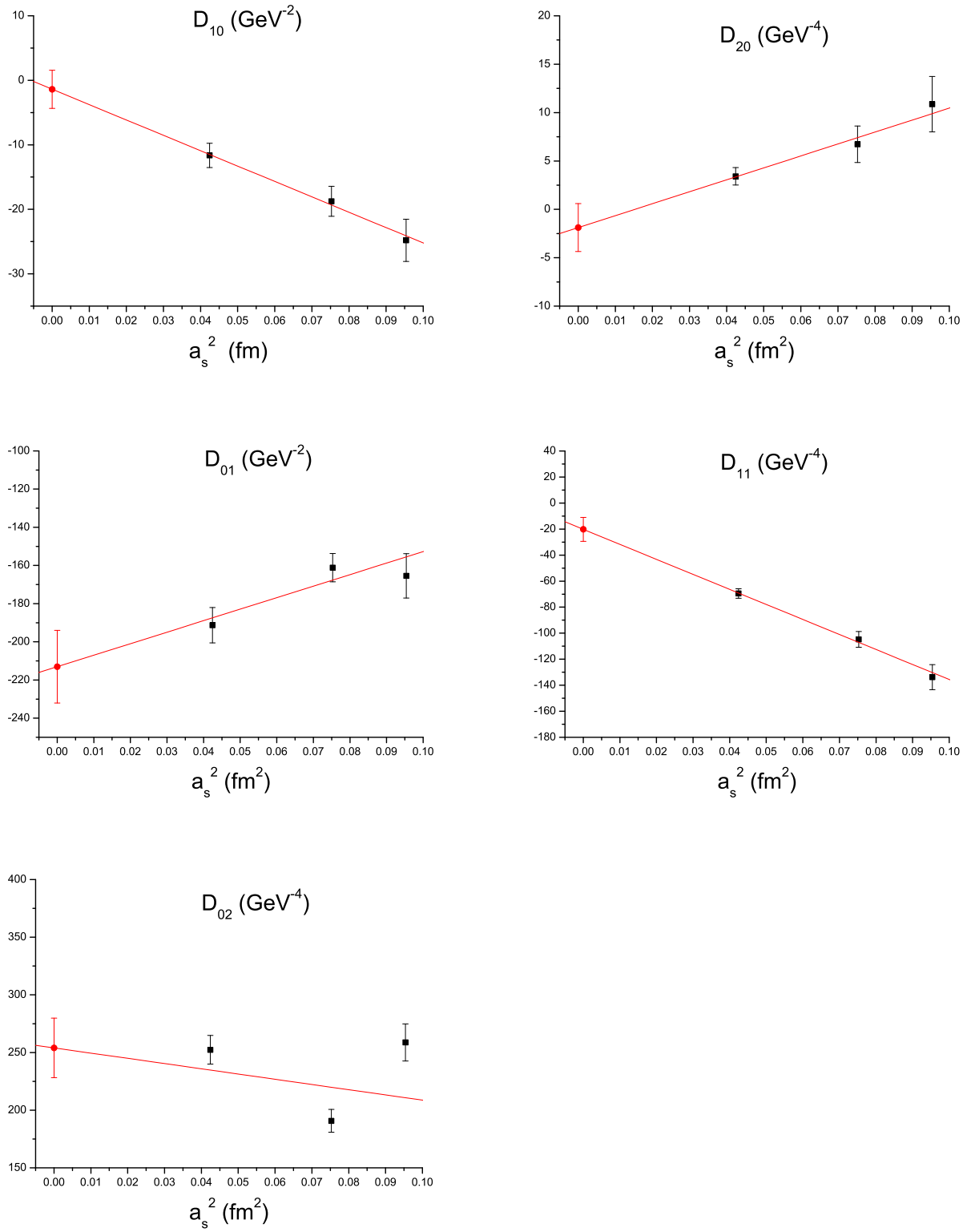


Fig. 5. The continuum limit extrapolation of the parameter  $D_{ij}$ . The solid circles near  $a_s = 0$  represent the corresponding continuum limit values.

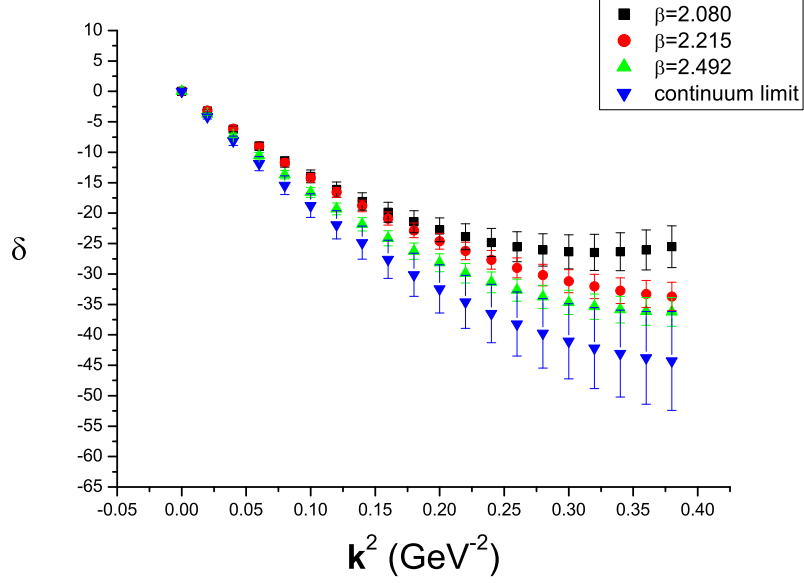


Fig. 6. The values of the phase shifts  $\delta$  after the chiral extrapolations at three values of  $\beta$ . The data points are labeled using squares, circles and triangles for three values of  $\beta$  respectively. Also shown are the continuum limit results of the phase shift which are labeled by upside-down triangles.

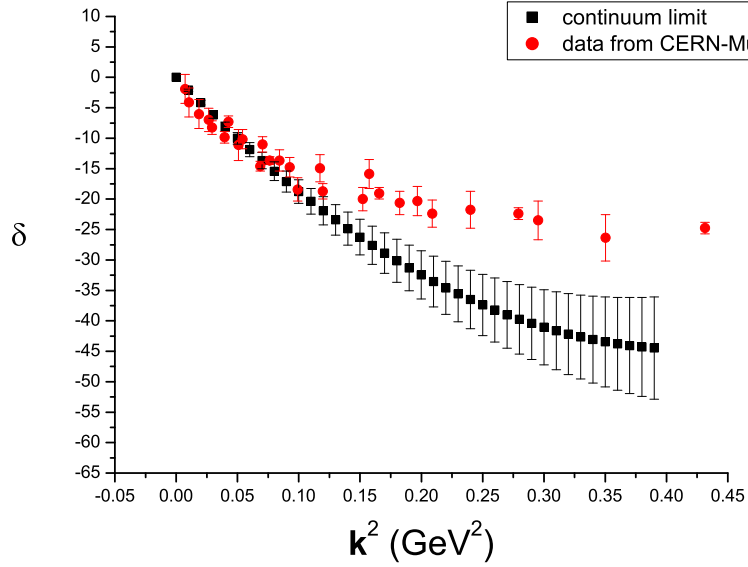


Fig. 7. Comparison of our lattice results for the scattering phase shifts with the experimental data from CERN-Munich [19]. Results are consistent with each other for  $\mathbf{k}^2$  below  $0.1 \text{ GeV}^2$  which roughly corresponds to the center of mass energy of about  $0.6 \text{ GeV}$ .